Journal of Macromolecular Science, Part A
Publication details, including instructions for authors and subscription information:
http://www.informaworld.com/smpp/title~content=t713597274

A Photochemical Approach to Integrated Optics

Harry D. Gafney[a]
[a] Department of Chemistry, Queens College City University of New York, Flushing, New York

To cite this Article Gafney, Harry D.(1990) 'A Photochemical Approach to Integrated Optics', Journal of Macromolecular Science, Part A, 27: 9, 1187 — 1202
To link to this Article: DOI: 10.1080/00222339009349685
URL: http://dx.doi.org/10.1080/00222339009349685

J. MACROMOL. SCI.—CHEM., A27(9–11), pp. 1187–1202 (1990)

A PHOTOCHEMICAL APPROACH TO INTEGRATED OPTICS

HARRY D. GAFNEY

Department of Chemistry
Queens College
City University of New York
Flushing, New York 11367

ABSTRACT

Highly resolved refractive index patterns or patterns of iron oxide are obtained by photolysis of $(CH_3)_3SnI$ or $Fe(CO)_5$ absorbed onto Corning's code 7930 porous Vycor glass followed by consolidation to a nonporous glass. The photochemistries of the molecules on the glass surface, as well as the distribution and relative sizes of the photodeposited metal oxides, are described. Rutherford backscattering, small-angle x-ray scattering, and scanning electron microscopy show that the glass consolidates about the iron oxide particle but not about the tin oxide particle. Tin oxide chemically modifies the glass surface so that it does not consolidate at temperatures as high as 1200°C.

INTRODUCTION

The development of the fiber optical waveguide for long distance signal transmission has been quite successful. However, full utilization of the technology depends on the development of optical circuitry [1, 2]. Optical circuits will require highly resolved refractive index patterns to guide the light through various active components. The active component itself may consist of highly resolved patterns of electrically or magnetically addressable materials, or materials capable of nonlinear optical phe-

nomena. Unfortunately, the refractory nature of glass fiber waveguides precludes simple coupling techniques. As a result, an optical circuit cannot be assembled, at present, in the same manner as an electronic circuit. Instead, the active and passive components must be integrated into the glass matrix. Consequently, optical circuitry hinges not only on the development of new photonic materials [3], but also on the development of procedures to incorporate precise patterns of these materials in glass.

One approach is a photolithographic technique in which organometallic reagents are photochemically bound to Corning's code 7930 porous Vycor glass (PVG), and the glass is thermally consolidated to a nonporous, nonscattering medium. For example, highly resolved patterns of gradient indices are obtained by photochemically binding $(CH_3)_3SnI$(ads) (ads designates an adsorbed species) to the glass matrix followed by thermal consolidation [4, 5]. Photolysis of $Fe(CO)_5$(ads) followed by thermal consolidation leads to equally well resolved patterns of iron oxide, principally magnetite [6]. Surprisingly, consolidation, which requires temperatures of $\geq 1000°C$ and in some cases reduces sample volume by as much as 25 to 35%, occurs with no detectable loss of pattern resolution [6].

With both compounds, photolysis binds the reagent to the glass matrix. Although the mechanisms by which this occurs vary, photoinduced binding was thought to be the key step to pattern resolution. Binding prevents migration and maintains pattern resolution during the thermal consolidation. Thermal consolidation, which requires temperatures of $\geq 1000°C$, volatilizes the unreacted adsorbate from the glass and converts the photoproduct to a metal oxide. The details of the latter reaction remain to be established. Yet, even if we assume the formation of a formal M—O bond (M being Fe or Sn, and O being a silanol oxygen) at some point during the reaction sequence, the above assumption is inconsistent with known bond energies [6].

The Sn—O bond energy, 132 kcal/mol [7], is considerably less than the Si—O bond energy, 185 kcal/mol [7]. These are average values, but it seems unlikely that the actual bond energy would differ by some 63 kcal/mol. Therefore, at the consolidation temperature, 1000°C, where there is sufficient energy, if not to break the Si—O bond certainly to weaken it so that consolidation to a nonporous glass occurs, we would expect that there is also sufficient energy to break the Sn—O bond. The discrepancy is more pronounced in understanding the resolution of the iron oxide images in the consolidated glass. Even if we again assume that a formal bond is formed between Fe and a silanol oxygen at some point during the

reaction sequence, the Fe—O bond energy, 92 kcal/mol [7], is only half that of the Si—O bond. At least energetically, photoinduced binding of the substrate to the glass, and most likely refractories in general, does not account for the observed pattern resolution [6].

The factors that control metal oxide pattern resolution lie in the underlying physical and chemical phenomena. To gain some insight into these factors, we have examined the nature of the glass itself, the photochemistries of $(CH_3)_3SnI$ and $Fe(CO)_5$ on the glass, and the aggregation and distribution of the metal oxides in the porous and consolidated glasses. Here, we summarize the results of these experiments.

POROUS VYCOR GLASS

Porous Vycor glass is a surface hydroxylated, transparent, porous glass composed of 96% SiO_2, 3% B_2O_3, and 1% Na_2O and Al_2O_3 [8–13]. When the melt is cooled, the boron-oxide–alkali-oxide phase separates, and acid leaching of the latter yields a myriad of precisely controlled pores interconnected throughout the glass in a random three-dimensional array. Small-angle x-ray scattering (SAXS) exhibits a broad peak (Fig. 1) around 0.018 1/Å, which corresponds to a correlation length of 23.2 nm

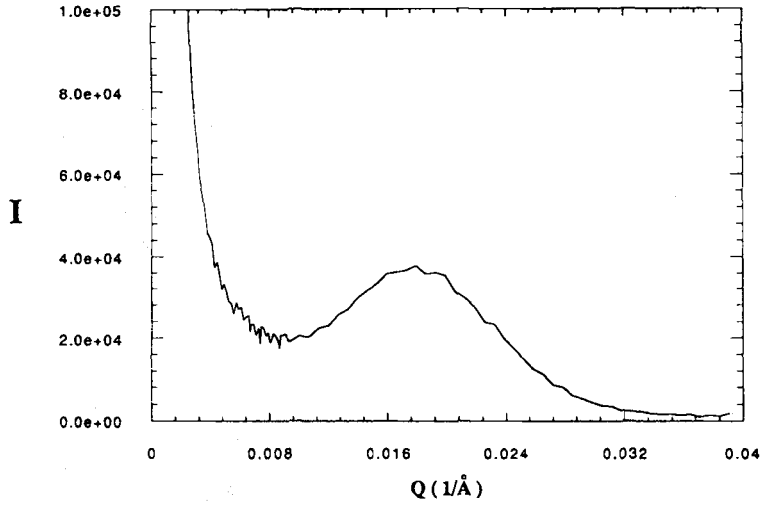

FIG. 1. Small-angle x-ray scattering from calcined (650°C) PVG.

[14]. These results agree with small-angle neutron scattering (SANS) which exhibits a scattering peak at 0.023 1/Å [15]. Each confirms a spinoidally decomposed, microporous material. Pore sizes are within the range of cavity sizes found in silica gels [10, 11], and both materials possess slightly acidic surface hydroxyls, i.e., silanol groups [12, 13], although the number/unit area depends on the extent of hydration and previous heatings. In many ways, PVG resembles silica gel, but one difference should be noted. Because of its method of manufacture, PVG possesses B_2O_3 Lewis acid sites [12, 13], although at this point whether these sites are involved in the observed chemistry is not known.

PHOTOCHEMISTRY OF IRON PENTACARBONYL AND IODOTRIMETHYLSTANNANE ADSORBED ONTO POROUS VYCOR GLASS

$Fe(CO)_5$ is used primarily as a photoactive precursor to magnetic adsorbates, principally Fe_3O_4 (magnetite), whereas $(CH_3)_3SnI$ is used as the precursor to tin oxide, which produces a transparent refractive index change in the glass. The choice is not intended to imply a single function, rather to illustrate the diversity of the chemistry in glass and the different effects caused by the photodeposited metal oxides.

Iron Pentacarbonyl

The appearance of the symmetric ν_1 mode, 2114 cm^{-1}, when the complex adsorbs onto PVG, indicates that some distortion occurs. Nevertheless, the similarity of electronic and IR spectra of $Fe(CO)_5$(ads) with the corresponding solution spectra, particularly the absence of lower energy ligand-field transitions, establishes that the complex physisorbs as a molecular entity without disruption of the primary coordination sphere [16].

Excitation of $Fe(CO)_5$(ads) *in vacuo* ($p \leq 10^{-4}$ torr) with light of ≤ 350 nm leads to CO evolution with a quantum efficiency of 0.96 ± 0.05 [16]. The electronic spectrum of the photoproduct is consistent with the formation of $Fe(CO)_4L$ species, but diffuse reflectance FTIR (DRIFT) spectra reveal the immediate appearance of two distinct, noninterconvertible photoproducts. These are assigned to $H-Fe(CO)_4-OSi$ and $H-Fe(CO)_4-OH$, where the primary photoproduct, $Fe(CO)_4$, oxidatively adds either a surface silanol group or chemisorbed water [16].

Continued photolysis leads to further decarbonylation and, depending on initial loading, excitation wavelength and intensity, and dimeric and trimeric analogs [16]. Each interacts with the glass surface to achieve some degree of stabilization, but this does not occur at the expense of subsequent thermal reactivity. All undergo rapid oxidation on exposure to air, although the nature of the oxide and its level of aggregation at this point are not presently known. If the photolysis is carried out in air, either the tetracarbonyl or its oxidative addition products undergo rapid oxidation [16].

Iodotrimethylstannane

Absorption spectra of $(CH_3)_3SnI$ in hexane consist of a single absorption with a maximum at 234 nm. A 254-nm photolysis of a degassed, hexane solution of $(CH_3)_3SnI$ leads to I_2 and $(CH_3)_3Sn-Sn(CH_3)_3$ formation [17]. The primary photochemical event is, as expected, homolytic cleavage of the Sn—I bond. The quantum efficiency of the process is 0.80 ± 0.02 with 254 nm excitation, but it declines to 0.22 ± 0.04 and ≤ 0.01 with 310 and 350 nm excitation, respectively. The wavelength dependence of the reaction, as well as the absence of lower energy emission and an O_2 dependence, point to the high energy state, populated on absorption, as the reactive state [17].

Photolysis of $(CH_3)_3SnI$ adsorbed onto PVG, however, is quite different, and the compound was examined in ethanol as a way of approximating the hydroxylated surface of the glass. When $(CH_3)_3SnI$ is dissolved in ethanol, the absorption maximum shifts to 219 nm. A 254-nm photolysis of a degassed ethanol solution of the compound does not result in I_2 or $(CH_3)_3Sn-Sn(CH_3)_3$ formation. Instead, HI is formed in a 1 : 1 stoichiometric ratio relative to the amount of $(CH_3)_3SnI$ decomposed. Conductance measurements indicate an immediate formation of ionic products, and IR and electronic spectra of the photolyte indicate that the tin photoproduct contains a bound CH_3CH_2O moiety [17].

When $(CH_3)_3SnI$ is adsorbed onto PVG, difference spectra show that the absorption maximum shifts to ≤ 220 nm. Irradiation of the sample *in vacuo* ($p \leq 10^{-4}$ torr) with 254 nm light causes spectral changes equivalent to those in ethanol, and HI is detected immediately in a 1 : 1 stoichiometric ratio [17].

Unlike most transition metal complexes, where the coordination sphere is fixed, R_3SnX and R_3PbX compounds react with Lewis bases to form 1 : 1 and 1 : 2 adducts [18]. Titrations of $(CH_3)_3SnI$ in hexane with *n*-

hexanol show that the shift in the absorption maximum from 234 nm in hexane to 219 nm in ethanol is due to the formation of an alcohol adduct, and Job's plots indicate a 1 : 1 adduct. FTIR spectra of the ethanol adduct are consistent with a five-coordinate species.

When $(CH_3)_3SnI$ is adsorbed onto PVG, the absorption maximum shifts to ≤ 220 nm. DRIFT spectra show a decline in intensity of the silanol band, 3755 cm^{-1}, and a concurrent growth of a broad O—H band centered at 3500 cm^{-1}. Although all PVG samples are calcined at 550°C prior to use, thermal gravimetric analysis and DRIFT spectra indicate the presence of small amounts of chemisorbed water [16]. Both chemisorbed water and the silanol groups are Lewis bases, and in principal, potential reaction sites. Since the spectral changes are independent of the extent of calcination, however, the dominant reaction appears to be with a silanol group to form a surface-bound five-coordinate adduct. The growth of the broad O—H band without the addition of water suggests that the complex does not formally displace the silanol hydrogen. Instead, the complex binds to the silanol oxygen, i.e.,

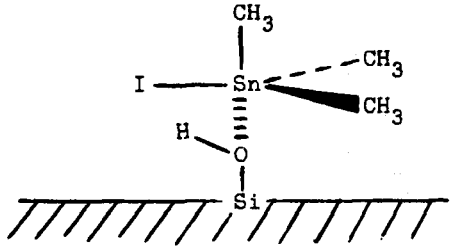

The interaction with the oxygen reduces the SiO—H bond strength and shifts the SiO—H band to lower frequency.

Addition of the silanol group not only increases the coordination number but also changes the electron distribution within the molecule. The specific nature of the electronic change is by no means clear, but the adduct is not a charge transfer complex *per se* [19]. The shift in the electronic absorption to higher energy, without a concurrent change in the 174-cm^{-1} Sn—I vibration, suggests that the major change occurs in the excited state. We believe that the addition of the Lewis base polarizes the Sn—I bond, and the increased polarization in the excited state switches the photochemical reaction from homolytic to heterolytic cleavage of the Sn—I bond. Photolysis releases I^- which then abstracts a proton to form HI and $(CH_3)_3Sn—OCH_2CH_3$ in ethanol, or $(CH_3)_3Sn—OSi$ (OSi denotes a surface silanol group) on the glass.

The quantum yield of the reaction in ethanol is 0.63 ± 0.05 with 254 nm excitation but reduces to 0.24 ± 0.03 on the glass surface. The wavelength dependence as well as the absence of an O_2 dependence suggests that the photoreaction in both media continues to occur from the high energy state populated on absorption. The smaller yield on the glass appears to be a consequence of the topology and rigidity of the glass surface. The reaction occurs within the crevises in the glass surface, and these irregularities enhance recombination by curtailing product separation. During consolidation, the surface-bound photoproduct is converted to tin oxide.

Establishing the reactive excited state points out the major drawback of $(CH_3)_3SnI$ and related analogs. The reactive excited state lies at high energy, and the optical absorptions populating the state occur beyond the UV-transmittance of the glass (50%T at 295 nm vs air). Consequently, the reactions and the resulting gradient index structures are limited to the outer glass surfaces. This is not to say that they are monolayer structures on a flat surface. The glass is initially porous and the surface topology allows some access into the bulk material. Cross-sectional x-ray micrographs (Fig. 2) show that, after consolidation, the tin oxide, and therefore the resultant gradient index structures, frequently have a depth on the order of hundreds of microns.

PATTERN CONTRAST AND RESOLUTION

This photolithographic technique is based on photochemically binding the reagent to the glass surface, converting the photoproduct to a metal oxide during thermal consolidation, and volatilizing the unreacted adsorbate from the glass [6]. Therefore, pattern contrast depends on the relative amounts of metal oxide in the photolyzed and unphotolyzed regions. In samples initially containing 10^{-4} mol $(CH_3)_3SnI/g$, photolyzed with 254 nm light and heated to 650°C to remove the unreacted adsorbate, the amount of tin near the surface of the photolyzed region (Fig. 2) is approximately an order of magnitude larger than that in unphotolyzed regions. Nevertheless, a significant amount of Sn remains in the unphotolyzed regions, thereby reducing pattern contrast. On the other hand, in an iron oxide image (Fig. 3), very little iron is found in the unphotolyzed regions of samples prepared under equivalent conditions, i.e., 10^{-4} mol $Fe(CO)_5/g$, photolyzed with 254 nm light and heated to 650°C to remove the unreacted adsorbate. With both complexes the amount of metal oxide in the photolyzed regions relative to that in the unphotolyzed regions

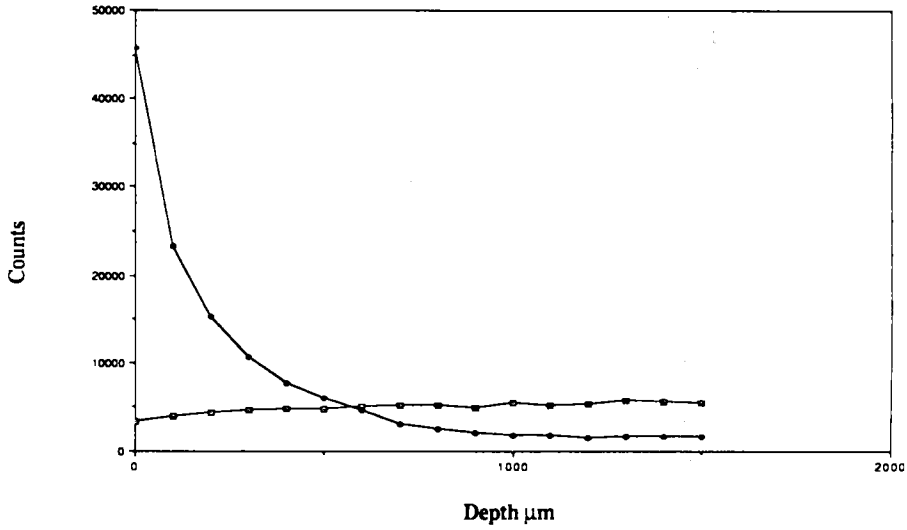

FIG. 2. X-ray analysis of the cross-sectional distributions of tin in the photolyzed (-♦-) and unphotolyzed (-⊡-) regions after heating to 650°C.

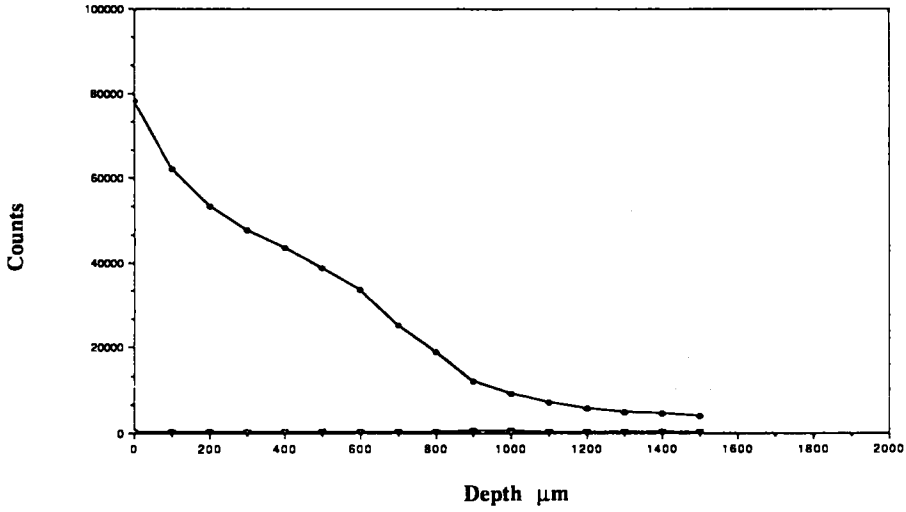

FIG. 3. X-ray analysis of the cross-sectional distributions of iron in the photolyzed (-♦-) and unphotolyzed (-⊡-) regions after heating to 650°C.

increases with increasing initial loading, but at all loadings the difference obtained with $Fe(CO)_5$ is significantly better than that obtained with $(CH_3)_3SnI$. This appears to be due to two factors. First, the larger fraction of the exciting light absorbed and the higher quantum efficiency of reaction of $Fe(CO)_5$(ads) yields a higher iron oxide content in the photolyzed regions relative to that obtained with $(CH_3)_3SnI$(ads). Second, $Fe(CO)_5$ physisorbs onto the glass, and this relatively weak interaction is readily overcome during subsequent heating. $(CH_3)_3SnI$ reacts with the glass surface to form a five-coordinate species. Apparently, coordination to the surface curtails desorption so that a larger fraction of $(CH_3)_3SnI$(ads) undergoes thermal oxidation during heating, thereby reducing pattern contrast.

Visually or under low magnification, the resolution of 25 mm × 25 mm × 1.4 mm metal oxide images of the periodic table in the consolidated glass [6], whether produced by photolysis of samples containing 10^{-4} mol $Fe(CO)_5$(ads)/g or 10^{-4} mol $(CH_3)_3SnI$(ads)/g, appear equivalent. However, more detailed analysis reveals startling differences. The iron oxide images (Fig. 4a) are grainy with small whiskers along the edges, whereas the tin oxide image (Fig. 4b) appears more uniform, almost cloudlike, with sharp, well-defined edges. Scanning electron microscopy (SEM) of the photodeposited metal oxides images shows a uniform distribution of relatively small tin oxide particles, whereas iron oxide appears as distinct, relatively large particles.

Particle size is related to, but is not simply a function of, initial loading. With samples containing $\sim 10^{-4}$ mol $Fe(CO)_5$(ads)/g, image formation is visually apparent during photolysis as a darkening in the exposed regions. SEM analysis of the consolidated sample shows that the image is composed of iron oxide particles that are on the order of 1 to 3 μm in diameter, and Mossbauer spectra indicate that the majority of the oxide is magnetite, Fe_3O_4. Secondary ion mass spectrometry (SIMS) (Fig. 5) shows that relatively little iron oxide is on the outermost surfaces of the consolidated glass. Instead, there is an overlying layer of glass $\sim$50 Å thick that contains little or no iron. At a depth of 50 Å there is a sharp rise in iron content and the amount present remains essentially constant to a depth of at least 4000 Å. Rutherford backscattering (RBS) (Fig. 6) shows that the particles exist in a substrate of uniform composition whose average stoichiometry over the first 0.5 μm, $SiO_2Fe_{0.2}$, corresponds to a consolidated glass containing a small amount of iron oxide.

As mentioned above, small-angle x-ray scattering (SAXS) from PVG yields a spectrum (Fig. 1) characteristic of a spinoidally decomposed

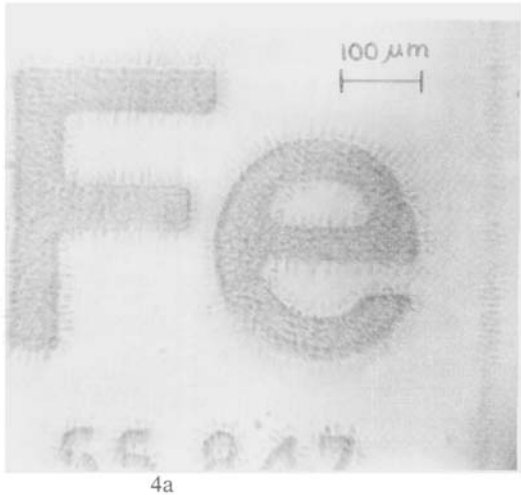

4a

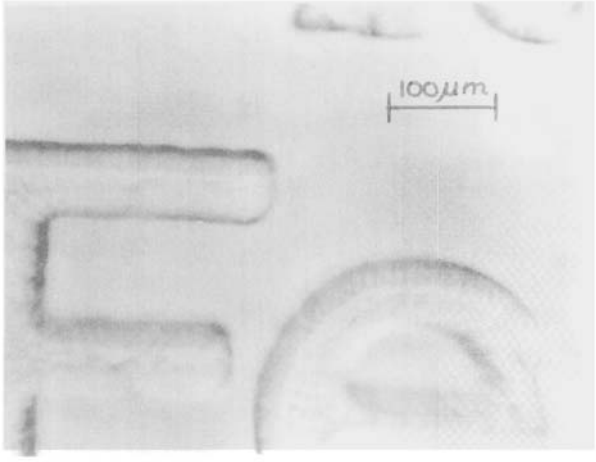

4b

FIG. 4. Enlargements (2000×) of photogenerated images composed of (a) iron oxide and (b) tin oxide after heating to 1200°C.

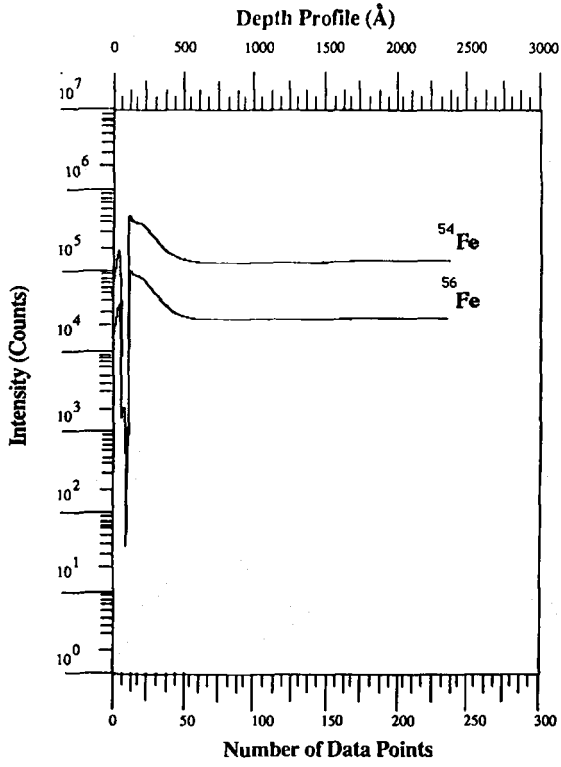

FIG. 5. SIMS analysis of the distribution of iron as a function of depth.

material with a correlation length of 23.2 nm. After heating to 1200°C, the peak corresponding to the different scattering centers disappears, indicating consolidation to a uniform, nonporous glass. Samples containing the photodeposited iron oxide exhibit identical changes. After heating to 650°C to remove the unreacted $Fe(CO)_5$(ads), the SAXS spectrum is equivalent to that of the unconsolidated glass (Fig. 1). Heating the sample to 1200°C results in a loss of the scattering peak. The resultant spectrum (Fig. 7) is equivalent to that of consolidated, unimpregnated PVG, and establishes that the iron oxide exists within a nonporous, uniform glass.

Photodeposition of tin oxide, on the other hand, produces quite different results. In contrast to the photodeposited iron oxide images, where opacity depends on initial loading, the photodeposited tin oxide remains

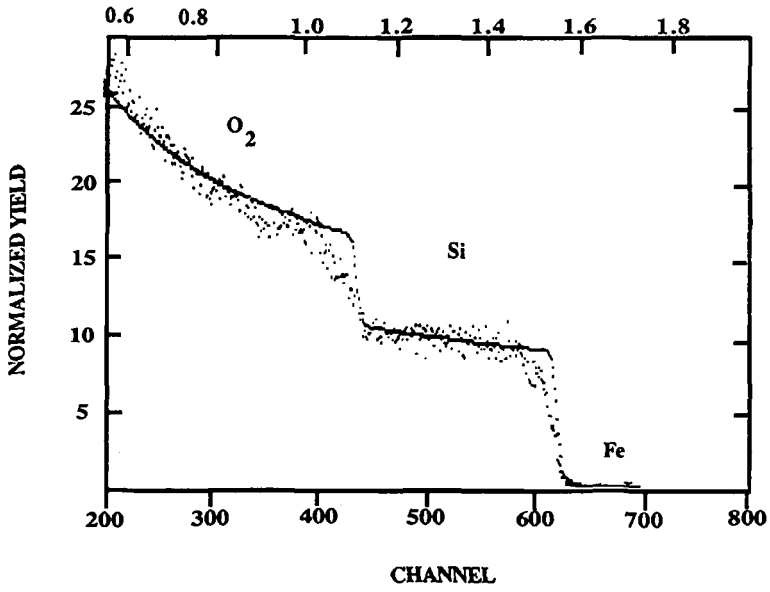

FIG. 6. Rutherford backscattering from samples containing photodeposited iron oxide after heating to 1200°C. Calculated (—) and observed (●) scattering.

transparent regardless of initial loading. RBS spectra of samples containing photodeposited tin oxide and heated to 1200°C (Fig. 8) differ from the calculated spectrum, which suggests that the tin oxide exists in a nonuniform, porous, or granular material. Also, the average stoichiometry over the first 0.5 μm of the consolidated sample is inconsistent with a uniform, fully consolidated glass in that there is an excess of oxygen relative to Si. Since PVG is hydroscopic and the samples were exposed to the open atmosphere, the excess oxygen is thought to be due to adsorbed water.

As in the $Fe(CO)_5$(ads) experiments, samples of PVG were impregnated with 10^{-4} mol $(CH_3)_3SnI$ and photolyzed with 254 nm light. After heating to 650°C to remove the unreacted material, SAXS spectra of the samples are equivalent to those of the unimpregnated porous glass (Fig. 1). However, heating the sample to 1200°C does not produce a change equivalent to those found with unimpregnated glass or with the glasses impregnated with iron oxide. In the regions containing the photodeposited tin oxide, SAXS (Fig. 9) continues to show a scattering peak which corresponds to a correlation length of 22.7 nm. SEM analysis of tin oxide

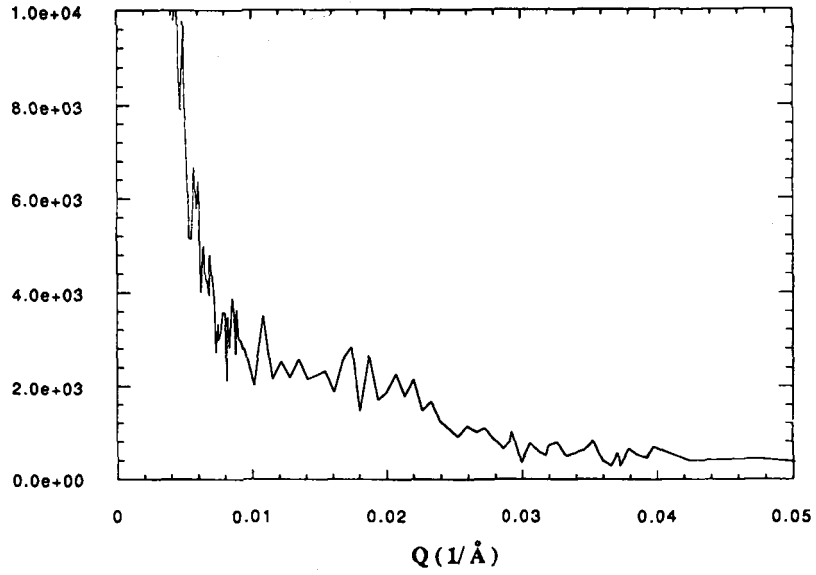

FIG. 7. Small-angle x-ray scattering from sample containing photodeposited iron oxide after heating to 1200°C.

impregnated regions shows that the surface has changed, but the impregnated regions are clearly porous. In other words, photodeposition of tin oxide prevents consolidation to a nonporous, uniform glass even at temperatures as high as 1200°C.

The lack of consolidation of the tin oxide impregnated regions is not simply due to metal oxide particle size. With both iron and tin oxides, the size of the photodeposited metal oxides increases with increasing precursor loading. Nevertheless, at each initial loading examined to date, which range from $\sim 10^{-6}$ to 10^{-4} mol/g, the resultant tin oxide particles are generally smaller than the iron oxide particles. Yet, the glass fully consolidates about iron oxide particles as large as 1 to 3 μm in diameter but does not consolidated, under equivalent conditions, about the smaller tin oxide particles. Rather, the lack of consolidation appears to be a chemical effect in which the tin oxide modifies the glass surface and prevents its consolidation. The mechanism by which this occurs, its dependence on the amount of tin deposited, or whether consolidation can be achieved at a higher temperature will be determined, but its effect on metal oxide imaging and its application to integrated optics are obvious.

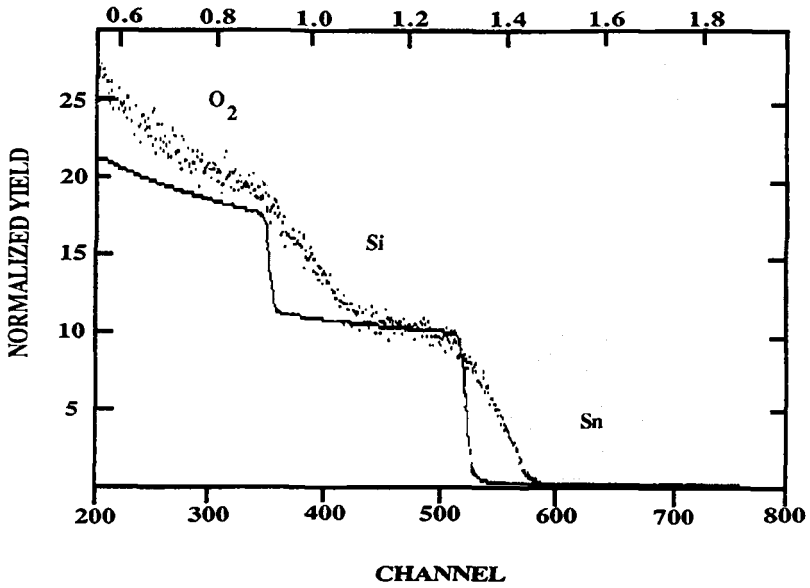

FIG. 8. Rutherford backscattering from samples containing photodeposited tin oxide after heating to 1200°C. Calculated (—) and observed (●) scattering.

The billowy, cloudlike appearance of the tin oxide images (Fig. 4b), as opposed to the graininess of the iron oxide images (Fig. 4a), is due to the fact that the tin prevents consolidation of the glass, whereas with the relative high loading used to produce a visible image, the iron exists as relatively large, distinct particles encapsulated within a consolidated glass matrix. Of course, the lack of consolidation precludes the use of tin oxide, and we suspect lead oxide, for photochemically generating longer optical waveguides because of light scattering. On the other hand, porosity offers access to the optic itself and removes the limitation imposed by the consolidation temperature of glass, i.e., the consolidation temperature limits impregnation to metals or metal oxides. This technique allows the maintenance of highly resolved, micron-sized regions of porosity in an otherwise consolidated glass sample. Experiments are in progress to determine if these porous regions can be impregnated in the same manner as PVG and whether it is possible to leach the tin from the region. We believe that these porous regions offer a means of incorporating into an integrated optical circuit a variety of reagents that were previously excluded because of an inability to withstand the consolidation temperatures.

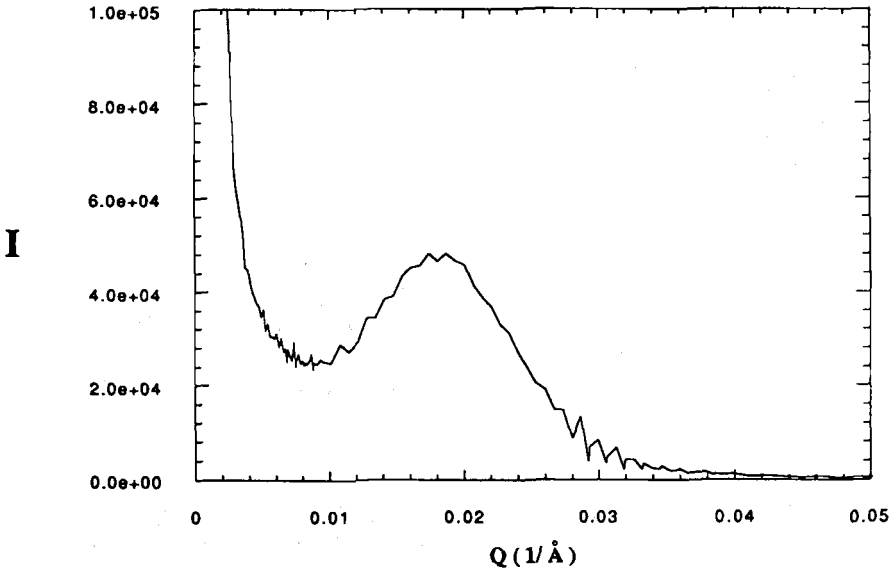

FIG. 9. Small-angle x-ray scattering from a sample containing photodeposited tin oxide after heating to 1200°C.

ACKNOWLEDGMENTS

The author thanks Mr. Edgar Mendoza and Mr. Eugene Wolkow for carrying out many of the experiments, Professor Miriam Rafailovich and Dr. Jonathan Sokolov of the Physics Department at Queens College for the RBS and SAXS analyses of PVG and the impregnated samples, and the Corning Glass Works for samples of porous Vycor glass. Support of this research by the Research Foundation of the City University of New York, the National Science Foundation (CHE-8913496) and the Office of Naval Research (N00014-87-K-0497) is also gratefully acknowledged.

REFERENCES

[1] S. E. Miller, "Integrated Optics, An Introduction," *Bell Syst. Tech. J., 48*, 2059, 2162, (1969).
[2] A. M. Glass, *Mater. Res. Soc., 12*(8), 14 (1988).
[3] E. M. Vogel, *J. Am. Ceram. Soc., 72*(5), 719 (1989).

[4] N. F. Borrelli, D. L. Morse, and J. H. Scheurs, *J. Appl. Phys., 54*, 6 (1983).
[5] N. F. Borrelli and D. L. Morse, *Ibid., 43*, 992 (1983).
[6] H. D. Gafney, *J. Imag. Sci., 33*, 37 (1989).
[7] Y. Yukawa, *Handbook of Organic Structural Analysis*, Benjamin, New York, 1965, pp. 544–545.
[8] T. H. Elmer, A. Felhner, and M. E. Nordberg, *J. Am. Ceram. Soc., 53*, 171 (1970).
[9] T. H. Elmer, I. D. Chapman, and M. E. Nordberg, *J. Phys. Chem., 66*, 1517 (1962).
[10] R. K. Iler, *The Chemistry of Silica*, Wiley-Interscience, New York, 1979, pp. 551, 622–714.
[11] V. F. Janowski and W. Heyer, *Z. Chem., 19*, 1 (1989).
[12] N. W. Cant and L. H. Little, *Can. J. Chem., 42*, 802 (1964); *43*, 1252 (1965).
[13] I. D. Chapman and M. L. Hair, *Trans. Faraday Soc., 61*, 1507 (1965); *J. Am. Ceram. Soc., 49*, 651 (1966).
[14] E. Mendoza, E. Wolkow, M. Rafailovich, J. Sokolov, and H. D. Gafney, *J. Appl. Phys.*, Submitted.
[15] P. Wiltzius, F. S. Bates, S. B. Dierker, and G. D. Wignall, *Phys. Rev., A, 36*, 2991 (1983).
[16] M. S. Darsillo, M. S. Paquette, and H. D. Gafney, *J. Am. Chem. Soc., 109*, 3275 (1987).
[17] E. Mendoza, D. L. Morse, and H. D. Gafney, Conference on Inorganic Chemistry, Harvard University, Cambridge, Massachusetts, 1987; Manuscript in Preparation.
[18] F. A. Cotton and G. Wilkinson, *Advanced Inorganic Chemistry*, 5th ed., Wiley-Interscience, New York, 1988, p. 292.
[19] S. Hoste, G. G. Herman, F. F. Roclant, W. Lippeus, and L. Verndock, *Spectrochim. Acta, 39A*(11), 959 (1983); *40A*(2), 215 (1984).